Composition and Physical Properties of Enceladus' Surface

Robert H. Brown[1], Roger N. Clark[2], Bonnie J. Buratti[3], Dale P. Cruikshank[4],

Jason W. Barnes[1], Rachel M. E. Mastrapa[4], J. Bauer[3], S. Newman[3], T. Momary[3],

K. H. Baines[3], G. Bellucci[5], F. Capaccioni[6], P. Cerroni[6], M. Combes[7], A. Coradini[6],

P. Drossart[7], V. Formisano[5], R, Jaumann[8], Y. Langevin[9], D. L. Matson[3],

T. B. McCord[10], R. M. Nelson[3], P.D. Nicholson[11], B. Sicardy[7], C. Sotin[12]

[1]Lunar and Planetary Laboratory, University of Arizona, Tucson, AZ 85721;

[2]U.S. Geological Survey, Denver, CO 80225

[3]Jet Propulsion Laboratory, Caltech, Pasadena, CA 91109

[4]NASA Ames Research Center, Moffett Field, CA 94035

[5]Instituto di Fisica dello Spazio Interplanetario, 0133 Rome, Italy

[6] Instituto di Astrofisica Spaziale, 0133 Rome, Italy

[7]Observatoire de Paris-Meudon, 92195 Meudon Cedex, France

[8]Deutsches Zentrum fuer Luft und Raumfahrt, 12489 Berlin, Germany

[9]Institute d'Astrophysique Spatiale, Universite de Paris, 91405 Orsay Cedex, France

[10]Department of Earth and Space Sciences, University of Washington, Seattle, WA 98195

[11]Astronomy Department, Cornell University, Ithaca, NY 14853

[12]University of Nantes, 44072 Nantes Cedex, France

Version of January 12, 2006

Abstract: Observations of Saturn's satellite Enceladus using Cassini's Visual and Infrared Mapping Spectrometer instrument were obtained during three flybys of Enceladus in 2005. Enceladus' surface is mostly nearly pure water ice except near its south pole, where there are light organics, CO_2, and amorphous and crystalline water ice, particularly in the region dubbed the "tiger stripes". An upper limit of 5 precipitable nm is derived for CO in the atmospheric column above Enceladus, and 2% for NH_3 in global surface deposits. The non-detection of NH_3 may have important implications for the chemistry of the Saturn system. Upper limits of 140 K (for a filled pixel) are derived for the temperatures in the tiger stripes.

Saturn's sixth largest satellite, Enceladus, orbits the planet within the extended E-ring at a distance of 238,020 km, or ~4 Saturn radii. Voyager images gave a reliable (equatorial) diameter of 513 km(*1*) and showed the surface to be a composite of moderately cratered terrain and large expanses with no craters. Internal activity has resulted in several episodes of resurfacing, ridge building, folding and faulting(*2, 3*). Near-infrared spectroscopy of Enceladus from Earth-based telescopes(*4-6*) has revealed partially crystalline H_2O ice, consistent with Enceladus' unusually high reflectance. At wavelength 0.8 μm the geometric albedo slightly exceeds 1.0(*5*). Some telescopic spectra show a weak absorption at 2.2-2.4 μm, suggestive of the presence of NH_3 or NH_3 hydrate(*4, 6*), while other spectra of similar quality do not(*5*). The spread in time of the spectra (1995 - 2003) and the change from an equatorial to a more south-polar view of Enceladus over that interval, suggest the possibility of short-term changes in the surface reflectance. Results of the Magnetometer investigation on Cassini gave early indications of a substantial atmosphere on Enceladus(*7*), which led to a lowering of the altitude of the July 14 flyby. The July 14 flyby led to the discovery of a plume of material emanating from the south-polar region of Enceladus, most likely from the tiger stripes (*8-11*). Areas within the tiger stripes are substantially hotter than would be expected if only passively heated by sunlight (*8*).

We report here near-infrared spectra of spatially resolved regions on Enceladus obtained using the Visible-Infrared Mapping Spectrometer (VIMS)(*12*) during the 3 Cassini flybys of this satellite in 2005 (February 17, March 9 and July 14, 2005). In total 207 VIMS cubes of Enceladus were obtained.

The VIMS is an imaging spectrometer operating in the wavelength region 0.35-5.2 μm in 352 channels, with a nominal pixel size of 0.5 mrad, and a maximum spatial format of 64x64 pixels. The data entity from the instrument is called a "cube" and can be thought of as a stack of 352,

64x64 images ordered by increasing wavelength.

The analysis of the VIMS data for Enceladus described in this paper is in 3 general areas: the composition of surface and the size of the ice grains in the near surface, the degree of crystallinity of the near surface, and the temperature of the surface. Although the analysis extended to the entire surface of Enceladus covered by the observations during the 3 flybys, we focus here on the south polar region of Enceladus and particularly on the area of the tiger stripes because they are so unusual.

Our analysis of the spectrum of Enceladus shows that its surface is almost completely dominated by water ice (Fig. 1) with a weak coloring agent in the UV-visible and with some minority constituents in specific areas as discussed below. Globally the typical water-ice grain size is 50 to 150 μm, but grain sizes increase to 100-300 μm in the tiger stripe regions (see Figs1 & 2).

We have found traces of free CO_2 ice, trapped CO_2 (either as a liquid or gaseous inclusion) and simple organics in the tiger stripes. While the organic signatures map geologic features (see Fig. 2), the close approach data for July 14 have anomalous noise that obscures spectral features beyond 4 μm. CO and CO_2 are molecules that could be expected to be found in icy bodies formed in the Saturn system(*13-18*), and indeed we find free CO_2 ice in small amounts globally, and in higher concentrations near Enceladus' south polar regions, but we see no CO (see below).

In data taken well before closest approach on 17 July, 2005, we see in the tiger-stripe region a strong signature of CO_2 with an absorption band depth of 74%. The center wavelength of the CO_2 absorption in the tiger-stripe region indicates that the CO_2 is not free ice but rather complexed, most likely with water ice (Fig. 3). There is no evidence in our data for free CO_2 ice in the tiger stripes. This is perhaps not surprising because the temperatures seen there by the

Cassini CIRS instrument(*8*) would cause solid CO_2 to rapidly migrate northward of the tiger stripe regions to areas with colder temperatures. Some free CO_2 is indeed seen northward of the tiger stripe region in our data. Furthermore, that there is such a high abundance of complexed CO_2 in the tiger stripe suggests active replenishment, probably from ongoing geophysical activity in the region(*8-11*).

No signature of CO ice, gas, clathrate, or in any other physical form was seen in our data. Based on the data taken about 1 hour before closest approach, an upper limit of 5 precipitable nm (corresponding to a column density of roughly 10^{14} molecules/cm^2) can be placed on the amount of CO in the atmospheric column above the tiger stripes.

Another cosmochemically important compound is NH_3. The role of NH_3 in solar system chemistry and geophysics has been extensively studied, and its role in Enceladus' geophysical activity widely hypothesized (*3, 19-23*). Unfortunately, no features due to NH_3 or its various hydrates were identified on Enceladus. To derive plausible upper limits for the abundance of NH_3 on Enceladus, we considered models of NH_3 + water ice mixtures. For NH_3 grain sizes similar to that of the water ice, we derive an upper limit of ~1%. If the NH_3-ice grains on Enceladus are larger than the water-ice grains, our modeling admits upper limits of ~3%. NH_3 has its strongest absorptions near strong water-ice absorptions, thus reducing the sensitivity of models where NH_3 is intimately mixed with water. It is possible that small areas of pure NH_3 exist if they subtend less than 10% of a VIMS pixel, but considering all of this, the likely global upper limit to ammonia on the surface of Enceladus is 2%. It should be noted, however, that as for CO_2, temperatures in the area of the tiger stripes may be high enough to cause free NH_3-ice to migrate northward to areas of lower temperatures.

There are many other apparent spectral features in the VIMS data for Enceladus that require

further study before an accurate assessment of their significance can be made. Of possible particular significance is a downturn beyond 5 μm and a possible 5.0-μm feature in the global average spectrum of Enceladus.

Disk-integrated spectra of Enceladus indicate that the water ice in Enceladus' equatorial and mid-to–high-latitude regions is primarily crystalline(*4, 6*). Nevertheless, amorphous water ice should exist on the satellite(*4*). Amorphous water forms when it is condensed directly from the vapor to a solid at temperatures below about 100K. If amorphous water ice is heated to 150 K it irreversibly and exothermally converts on timescales of minutes to hours to crystalline water ice. The conversion can only be reversed by disruption of crystal structure by bombardment of high energy particles(*24*)—a process primarily limited by dose rather than by the energy spectrum of the impacting particles(*25*). Examples of such a process can be seen on the Galilean satellites(*24, 26, 27*).

Enceladus orbits in the inner regions of Saturn's magnetosphere where the particle flux is quite high. Furthermore, Enceladus may have it's own magnetic field(*7*), which could increase the particle flux at its poles, making it prudent to look for amorphous ice near Enceladus' poles.

Differences in their spectra can be exploited to search for crystalline and amorphous ice on Enceladus (see Fig. 4). The two most obvious indicators are the 1.65-μm absorption band, and the 3.1-μm Fresnel reflection peak, both of which are much more prominent in crystalline ice. In addition, the central wavelengths of the absorption bands vary significantly between amorphous and crystalline water ice due to the reduced hydrogen bonding in amorphous water ice compared to crystalline (Fig. 4b). Our analysis indicates that, in a local sense (that is, confining our analysis to the south-polar regions of Enceladus) crystalline ice is most abundant in the tiger stripes, while amorphous ice is most abundant in the south-polar regions, outside the tiger stripes. This is

shown in the global ratio of the 1.2-μm reflectance to the 1.65-μm absorption band (Fig. 4c) and in the ratio of the 1.2-μm reflectance to the 3.1-μm peak (Fig. 4d), except that the tiger stripes are darker because the crystalline ice is brighter at 3.1 μm.

Laboratory experiments show that crystalline ice at temperatures below 100K rapidly converts to amorphous ice in the presence of high energy particles(*25*), and re-crystallizes very quickly when heated ~140-150 K(*24*). For geologically active, relatively hot areas like those near Enceladus' south pole it would be difficult, if not impossible, to determine the time that these materials have been exposed to magnetospheric bombardment; i.e., their age. If, on the other hand, areas with a high degree of crystallinity exist in the coldest areas in the south-polar region of Enceladus, they would be young, perhaps as young as a few decades(*25*). Further study of our data and additional observations of Enceladus' south-polar region are required to address the question of age.

Despite the unambiguous detection of anomalously hot areas on Enceladus by the Cassini CIRS instrument(*8*), VIMS did not detect thermal emission from within the tiger stripes, mostly because the cutoff wavelength of the instrument is 5.2 μm. Co-adding spectra of the stripes to improve S/N allows us to place a robust 3-sigma upper limit at 140K on the average temperature of VIMS tiger stripe pixels(*28*). Alternatively, a swath within the stripes can neither be wider than 135 meters at the ammonia-water eutectic temperature of 173K nor wider than ~20 centimeters at the water triple point 273K!

Figure 1a-1d: Spectra of Enceladus in the region of the tiger stripes and from nearby regions. (a) illustrates the tiger-stripe region and the areas from which the two averaged spectra are taken. (b) shows the full I/F spectra of the two regions obtained by averaging all of the individual spectra in

the tiger stripes and in the immediate areas as indicated in the top panel and as color coded. (c) shows a blowup of the 3.0- to 5.2-μm spectral region. (d) shows the ratio of the two spectra blown up in the 3.3- to 4.1-μm spectral region. The error bars in (d) result primarily from level shifts in the two spectra as the tiger stripes are noticeably darker than the surrounding regions. The actual uncertainty in the spectra is better represented by the point-to-point scatter. Note the absorptions near 3.44 & 3.53 μm in the ratio spectrum in (c) that we attribute to short-chain organics. There are other features in the ratio spectrum which may be real and are, as yet, unidentified. Note that all spectra shown have no units. They are simple numerical ratios.

Fig. 2: A compositional map of Enceladus. This map was produced by stacking red, green and blue images coded as follows: the red image maps the strength of the 3.44-μm organic absorption to red intensity, the green image maps the 2.2-μm continuum reflectance to green intensity, and the blue image maps the intensity of the 3-μm water ice absorption to blue intensity. The images are then stacked as a red-green-blue triplet. Note the correlation of the organic signature with the tiger stripes, and the presence of stronger water-ice absorptions there as well.

Fig. 3: Average spectrum of the tiger stripes. Note the strong CO_2 absorption near 4.26 μm. The two curves labeled 150K and 140 K are the apparent reflectance that would result for a surface having a 0.0 actual reflectance at the temperatures indicated.

Fig 4a-4d: (a) Spectra of crystalline and amorphous ice, showing the 1.6-μm absorption band and the 3.1-μm Fresnel peak, both characteristic of crystalline ice (4). (b) VIMS co-added spectra of the "tiger stripes" and the south-polar region between the tiger stripes. Below the graph are the band positions for the main absorption bands at 1.5 and 2.0 μm and the Fresnel peak at 3.1 μm for the tiger stripes, the region between the tiger stripes, and amorphous and crystalline ice. The region with spectral characteristics most similar to crystalline ice is the tiger stripes. (c) A ratio of the 1.2-μm continuum to the 1.65-μm crystalline ice absorption band, showing that the tiger stripes have the deepest absorption at 1.65-μm and thus have the highest abundance of crystalline ice. (d)) A ratio of the 1.2-μm continuum to the 3.1-μm Fresnel peak characteristic of crystalline water ice. The peak is highest in the tiger stripes, which is consistent with a high degree of crystallinity. (The dark regions in the left part of the mosaics in part (c) and (d) are due to saturated data.)

Reference List

1. B. A. Smith *et al.*, *Science* **215**, 504 (1982).
2. W. B. McKinnon, *Reviews of Geophysics* **25**, 260 (1987).
3. J. S. Kargel, S. Pozio, *Icarus* **119**, 385 (1996).
4. W. M. Grundy, M. W. Buie, J. A. Stansberry, J. R. Spencer, B. Schmitt, *Icarus* **142**, 536 (1999).
5. D. P. Cruikshank *et al.*, *Icarus* **175**, 268 (2005).
6. J. P. Emery, D. M. Burr, D. P. Cruikshank, R. H. Brown, J. B. Dalton, *Astronomy & Astrophysics* **435**, 353 (2005).
7. M. K. Dougherty, et al, *Science* **this issue**, XX (2005).
8. J. R. Spencer, et al, *Science* **this issue**, XX (2005).
9. C. J. Hansen, et al, *Science* **this issue**, XX (2005).
10. J. H. Waite, et al, *Science* **this issue**, XX (2005).
11. C. C. Porco, et al., *Science* **this issue**, ?? (2005).
12. R. H. Brown *et al.*, *Space Science Reviews* **115**, 111 (2005).
13. J. S. Lewis, *Icarus* **15**, 174 (1971).
14. J. S. Lewis, *Science* **172**, 1127 (1971).
15. J. S. Lewis, *Scientific American* **230**, 51 (1974).
16. J. S. Lewis, *Annual Review of Physical Chemistry* **24**, 339 (1973).
17. J. S. Lewis, R. G. Prinn, *Astrophysical Journal* **238**, 357 (1980).
18. J. S. Lewis, *Science* **186**, 440 (1974).
19. D. J. Stevenson, J. Bergstrahl, Ed. 1984), pp. 405-424.
20. D. J. Stevenson, *Nature* 142 (1982).
21. S. W. Squyres, R. T. Reynolds, P. M. Cassen, S. J. Peale, *Icarus* **53**, 319 (1983).

22. J. S. Kargel, *Earth Moon and Planets* **67**, 101 (1995).

23. R. G. Prinn, B. Fegley, *Astrophysical Journal* **249**, 308 (1981).

24. G. B. Hansen, T. B. McCord, *Journal of Geophysical Research-Planets* **109**, (2004).

25. G. Strazzulla, G. A. Baratta, G. Leto, G. Foti, *Europhysics Letters* **18**, 517 (1992).

26. M. G. Kivelson *et al.*, *Nature* **384**, 537 (1996).

27. G. Schubert, K. K. Zhang, M. G. Kivelson, J. D. Anderson, *Nature* **384**, 544 (1996).

28. To extablish upper limits on temperature, we used a Levenberg-Marquardt algorithm to fit the co-added tiger stripe spectrum to the spectrum of the interstripe region using a multiplicative albedo-surrogate scaling factor and surface temperature as free parameters. The best-fit temperature is indistinguishable from 0 K. We then increased the temperature of either the full pixel or a linear swath through the pixel until the quality of the fit degraded to the 3-sigma level, and used that value for the upper limit.

29. The authors acknowledge funding from the U.S. National Aeronautics and Space Administration.

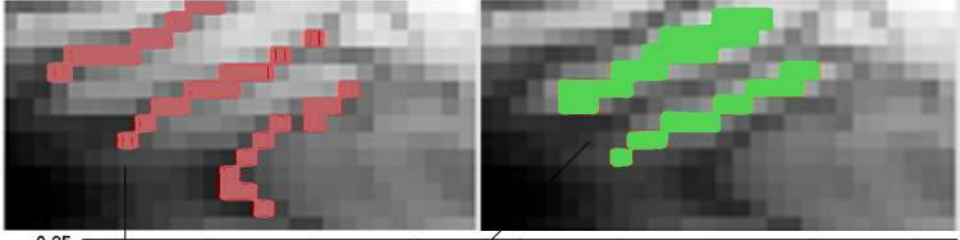

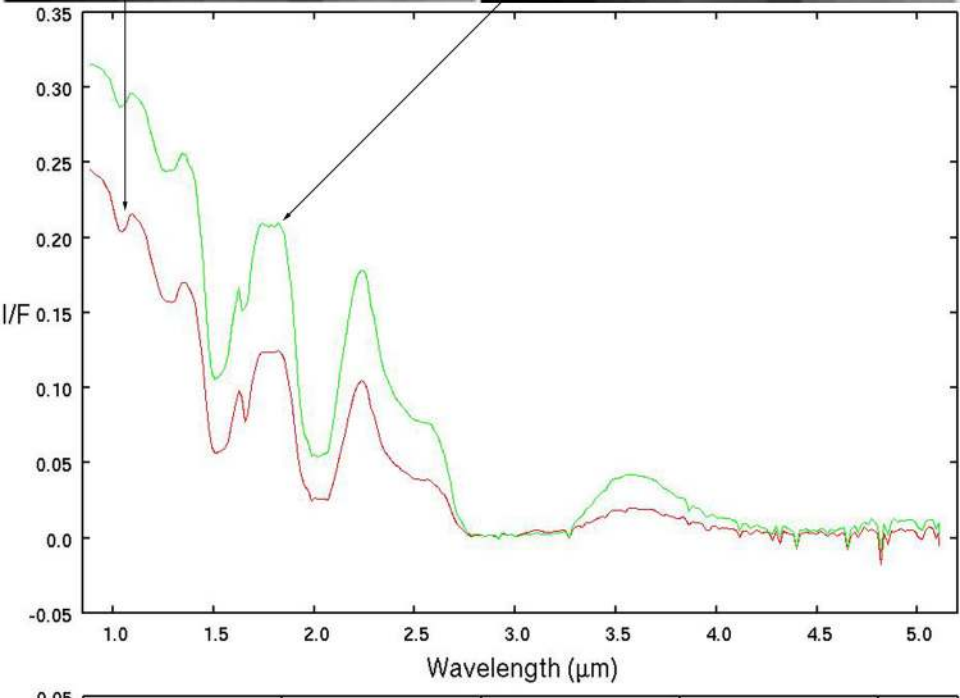
I/F
Wavelength (μm)

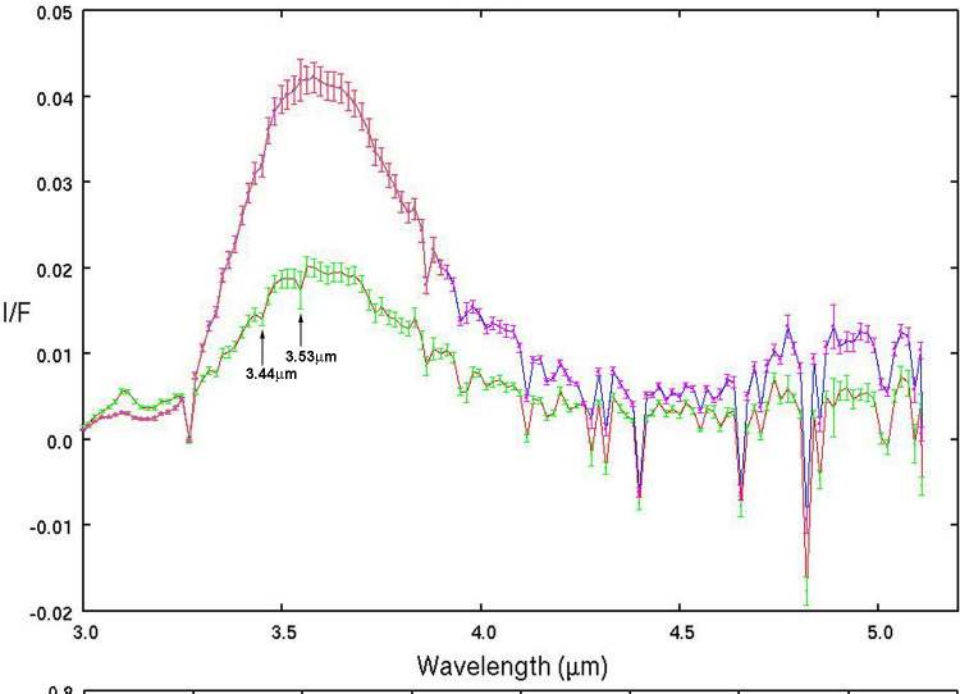
I/F
3.44μm
3.53μm
Wavelength (μm)

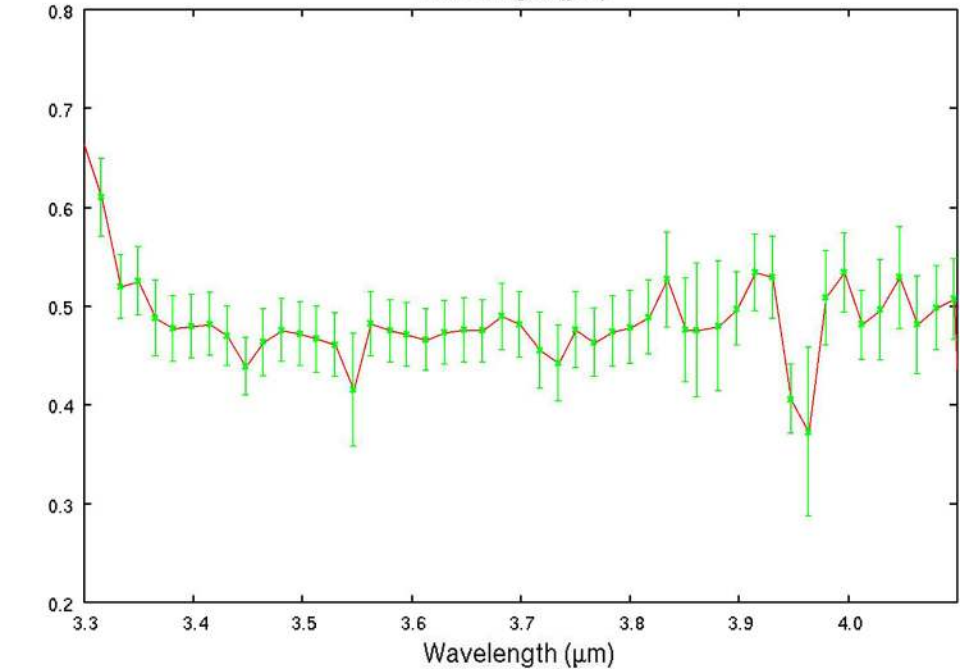
Wavelength (μm)

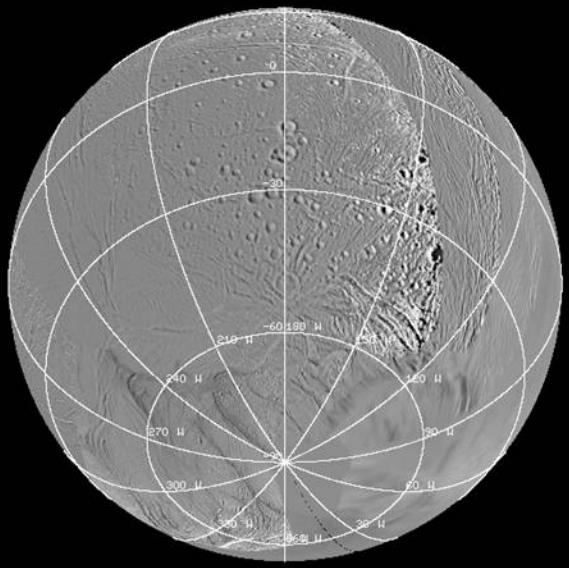

ISS Reference

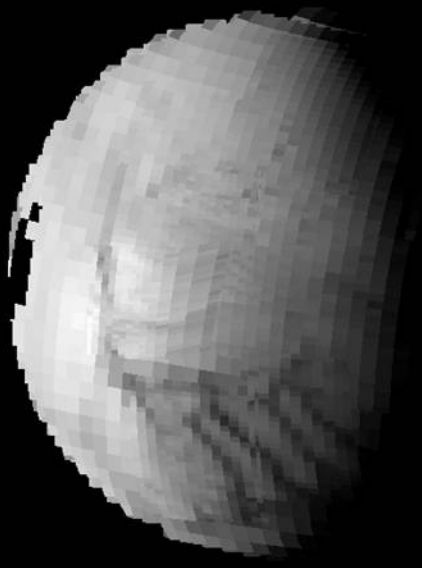

2.2-micron Reflectance

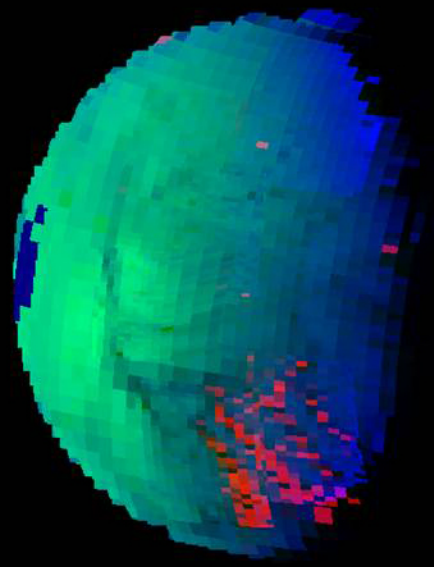

Color Composite

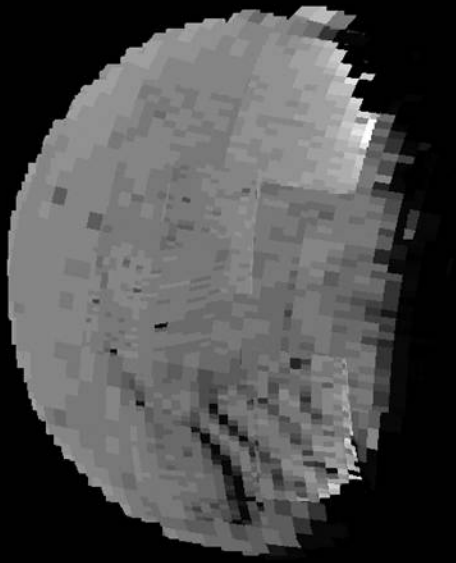

3-micron Ice
Absorption Strength

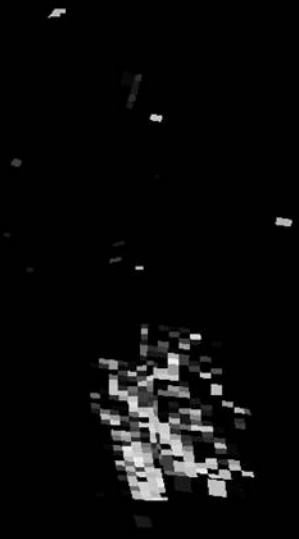

3.44-micron Organic
Absorption Strength

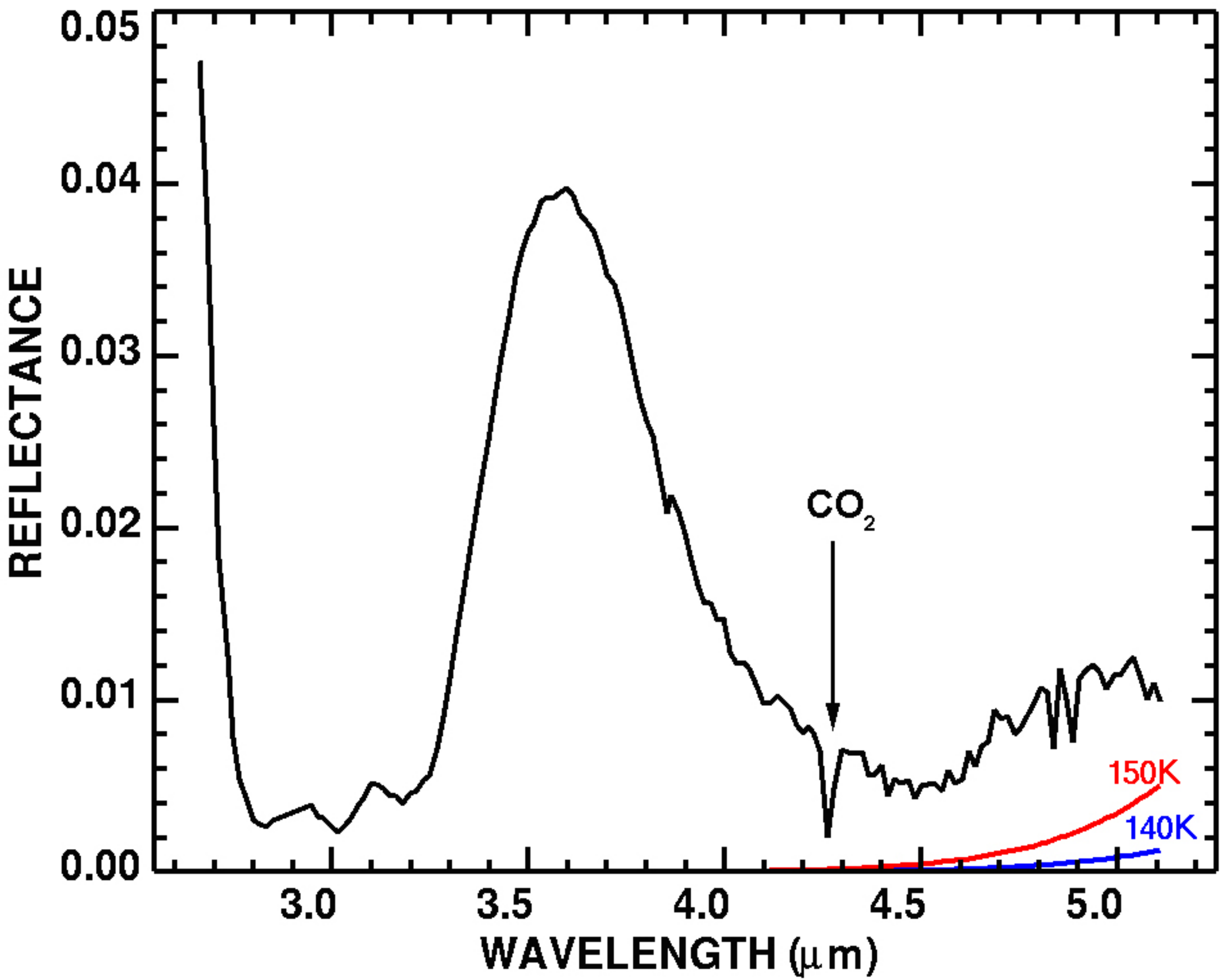
0.05
0.04
0.03
0.02
0.01
0.00
REFLECTANCE
3.0
3.5
4.0
4.5
5.0
WAVELENGTH (μm)
CO2
150K
140K

a.

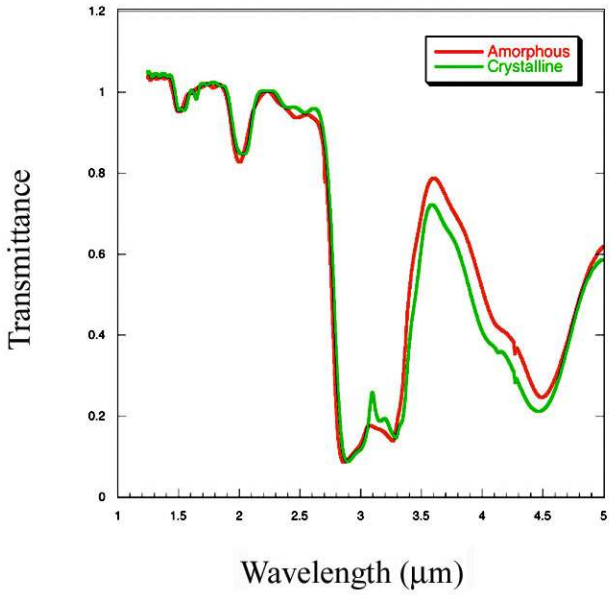
Amorphous
Crystalline
Transmittance
Wavelength (μm)

b.

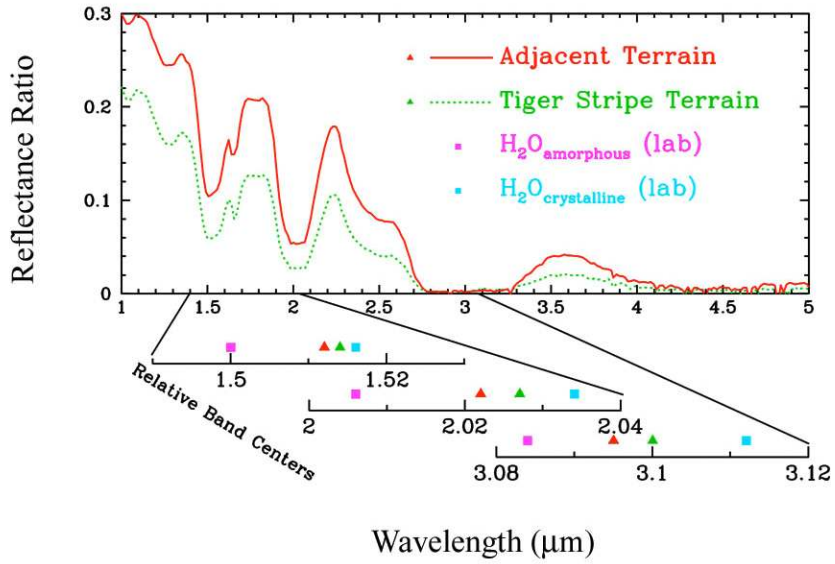
Adjacent Terrain
Tiger Stripe Terrain
H2Oamorphous (lab)
H2Ocrystalline (lab)
Reflectance Ratio
Relative Band Centers
Wavelength (μm)

c.

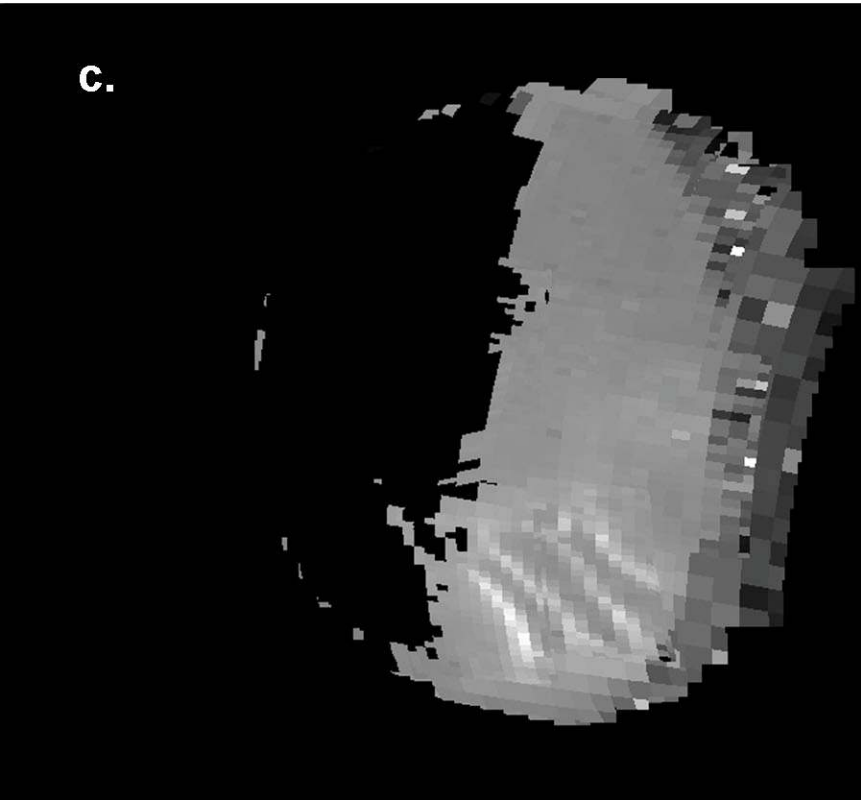

d.